

Structure and Dynamics in Solution of Bis(phenoxy-amine)Zirconium Catalysts for Olefin Polymerization

Gianluca Ciancaleoni,^{†,‡} Natascia Fraldi,^{‡,§} Peter H. M. Budzelaar,^{*,||} Vincenzo Busico,[§] and Alceo Macchioni^{*,†}

[†]Dipartimento di Chimica, Università di Perugia, via Elce di Sotto, 8, 06123 Perugia, Italy

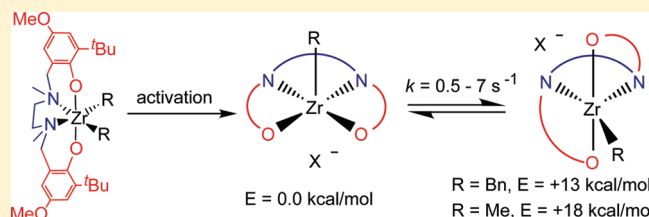
[‡]Dutch Polymer Institute (DPI), P.O. Box 902, 5600 AX Eindhoven, The Netherlands

[§]Dipartimento di Chimica, Università di Napoli Federico II, Via Cintia, 80126 Napoli, Italy

^{||}Department of Chemistry, University of Manitoba, Winnipeg, Manitoba R3T 2N2, Canada

S Supporting Information

ABSTRACT: The activity of two bis(phenoxy-amine)ZrR₂ precatalysts (bis(phenoxy-amine) = *N,N'*-(3-*t*-Bu-5-OMe-2-C₆H₂OCH₂)₂-*N,N'*-Me₂-(NCH₂CH₂N)); R = Me (**1**), Bn (**2**, benzyl)) toward propene polymerization has been evaluated using different activators and cocatalysts: MAO, MAO/TBP, B(C₆F₅)₃/TIBA, and [CPh₃][B(C₆F₅)₄]/TIBA (MAO = methylalumoxane, TBP = 2,6-di-*tert*-butylphenol, TIBA = triisobutylaluminum). It was found that the nature of the activator affects the activity only to a small extent. NMR studies in solution and DFT calculations on the **3a**–**c** and **4a**–**c** (**a**, MeB(C₆F₅)₃[−]; **b**, BnB(C₆F₅)₃[−]; **c**, B(C₆F₅)₄[−]) ion pairs deriving from the activation processes of **1** and **2**, respectively, showed that three isomers can form. All of them have the anion in the second coordination sphere, whereas the binding modality of the ligand leads to the *mer-mer* most stable isomer, *fac-mer* isomer of intermediate stability, and *fac-fac* least stable isomer. Notably, the energy of the *fac-fac* isomer, which is supposed to be the active species in the polymerization process, depends more on the R group and not much on X[−], in agreement with the small influence of the activators on the polymerization activity.



INTRODUCTION

In recent years, a significant effort has been devoted to the discovery of new postmetallocene α -olefin polymerization catalysts and rationalization of their performance on the basis of their structures.¹ Tetradentate bis(phenolate) ligands of the type [OYYO] (Y = heteroatom donor N,² P,³ S⁴, or O⁵) have attracted interest because they might mimic the steric environment of the surface Ti atoms in classical heterogeneous Ziegler–Natta systems used for industrial production of isotactic polypropylene.⁶ Furthermore, the steric and electronic properties of the [OYYO] ligands can be easily modulated, also taking advantage of the high-throughput parallel screening technologies.⁷ From a catalytic point of view, the [ONNO] bis(phenoxy-amine)^{2a,8} class of complexes generally shows low activity and high isotacticity for 1-hexene and propene polymerization,^{2a,9} although higher activities can be obtained by ligand modification^{10a} or with different monomers, such as *rac*-lactide.^{10b}

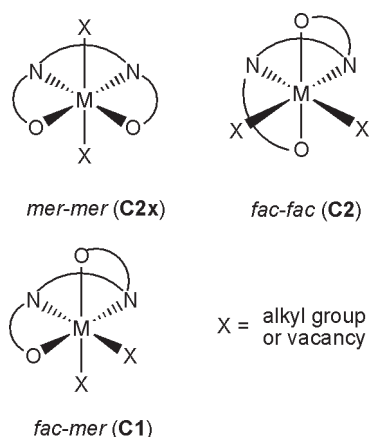
The structures of complexes bearing the bis(phenoxy-amine) ligand are rather diverse, since the inherent flexibility of the ligand backbone allows several coordinative geometries to be adopted. For example, the ligand disposition is intermediate between square pyramidal and trigonal bipyramidal in five-coordinated aluminum complexes;¹¹ a *fac-mer* geometry (Scheme 1) is preferred with octahedral chromium(III),¹² while a tetrahedral arrangement is adopted with manganese(II).¹³ With group 4

metals, the ligand wraps the octahedral metal center in a *fac-fac* mode (Scheme 1), leading to the C₂-symmetrical neutral precursors (ONNO)MR₂ (R = Bn,^{2a,7} Me₂CHO^{8a,10}).¹⁴ This has been confirmed by both X-ray crystallography and ¹H NMR spectroscopy.^{2a} Much less is known about the ligand conformation after activation, since the resulting ion pair is often not stable^{2a} or exhibits significant dynamic behavior, precluding an accurate NMR study.¹⁵

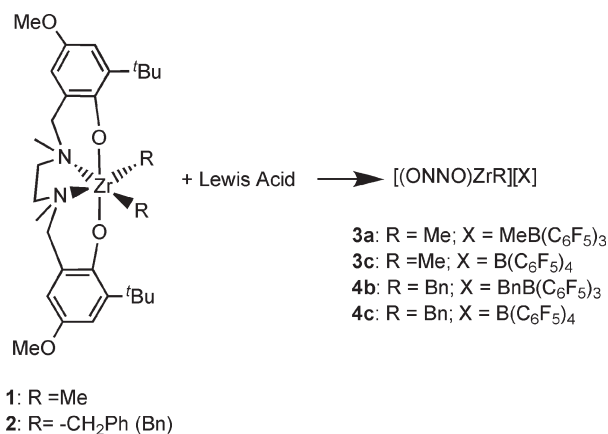
In one case the structure of a bis(phenoxy-amine)zirconium ion pair was fully elucidated.¹⁶ Particularly, NMR and DFT (density functional theory) studies were carried out for the [(*N,N'*-(3-CMe₂Ph-5-Me-2-C₆H₂OCH₂)₂-*N,N'*-Me₂-(NCH₂CH₂N))ZrMe]-[MeB(C₆F₅)₃] (**5a**) ion pair, which is a competent catalyst for olefin polymerization.⁷ It was found that the most stable isomer in solution is the outer-sphere ion pair (OSIP)¹⁷ *cis*(*N,N*)-*cis*(*O,O*) (C2x,¹⁸ or *mer-mer*, Scheme 1), with a distorted-square-pyramidal geometry, having the Zr–Me bond in an apical position and the anion on the opposite side. If **5a** were exclusively present as the C2x isomer, it would be inactive in polymerization, since the entering olefin would be trans to the alkyl chain and the insertion could not take place. This led us to hypothesize that the C2x isomer transforms into the *cis*(*N,N*)-*trans*(*O,O*) (C2, or

Received: March 1, 2011

Published: May 02, 2011

Scheme 1. Geometrical Isomers of [(ONNO)ZrX₂] Complexes

Scheme 2. Syntheses and Numbering of Ion Pairs



fac-fac) isomer having all the correct features to be the active species for the polymerization of olefins.⁷ Consistent with this hypothesis, we recently showed that only the inclusion of the C2_x-C2 isomerization process in the reaction pathway of propene polymerization, mediated by a bis(phenoxy-amine)-ZrBn₂ complex, allows the experimental kinetic parameters to be well reproduced by DFT calculations.¹⁹

In this work, we explore the scope of such an unusual reaction pathway by investigating the influence of the activator on the ion pair structure and catalytic performance. For this purpose, ion pairs **3a,c** and **4b,c** were synthesized from precursors **1** and **2** (Scheme 2), fully characterized both experimentally (¹⁹F, ¹H-HOESY, ¹H-EXSY, and ¹H-PGSE NMR studies) and computationally (DFT calculations) and tested in the polymerization of propene.

RESULTS AND DISCUSSION

Polymerization Tests. Catalyst precursors **1** and **2** were tested in the polymerization of propene in toluene, using different activators and cocatalysts: MAO (MAO = methylalumoxane),^{20–22} MAO/TBP (TBP = 2,6-di-*tert*-butylphenol),²³ B(C₆F₅)₃/TIBA (TIBA = triisobutylaluminum),²⁴ and [CPh₃][B(C₆F₅)₄]/TIBA.^{23,25} The results are shown in Figure 1. In all cases the

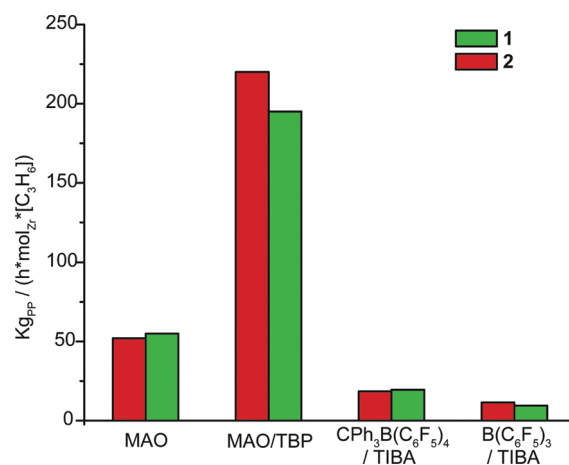


Figure 1. Dependence of catalyst productivity on the choice of activator.

productivity is quite low,⁹ less than 250 kg_{pp}/(h mol_{Zr} [C₃H₆]), indicative of an inherent slowness of the catalyst toward propene.¹⁸ The three boron-based anions give essentially the same very low productivity (Figure 1), around 10–20 kg_{pp}/(h mol_{Zr} [C₃H₆]), independent of the precise choice of the anion.

These results are anomalous if compared with those for the archetypal metallocene catalysts, where there is a large influence of the activator on the productivity:²⁶ the use of [CPh₃][B(C₆F₅)₄] instead of B(C₆F₅)₃ usually leads to a 200-fold increase in propene polymerization productivity, even in the presence of TIBA.²³ This difference has been attributed to the different coordinating abilities of B(C₆F₅)₄[−] and MeB(C₆F₅)₃[−], implying that the energy cost of displacement of the counterion contributes to the rate-limiting step. In the present case, the increase is small and is believed to be within experimental error, giving us an important piece of information about the polymerization mechanism: displacement of the anion is not part of the rate-determining step and may even not be involved at all in the mechanism (see below). The use of MAO alone results in only a modest increase in activity (by a factor of about 2); a larger increase in productivity (factor of 10) can be achieved by combining MAO with TBP (Figure 1).²² This still corresponds to a rather modest change in activation energy.

In a paper by Kol and co-workers about similar catalyst precursors, having chlorine atoms on the phenol ring, it was shown that also a change of solvent did not substantially alter the 1-hexene polymerization activity.^{8a} The same group reported that, for 1-hexene polymerization using catalyst precursors based on a C₁-symmetric (ONNO')Zr framework,^{10a} the isotacticity and polymer molecular weight were unaffected by the activator used to generate the active species. The independence of the catalytic parameters on the anion and activation conditions appears to be a general issue for the bis(phenoxy-amine)-based catalysts. For this reason, a more detailed comprehension of the structure and dynamics of the resulting active species in solution is desirable.

Syntheses and Characterization of Ion Pairs in Solution.

The reactions of precursors **1** and **2** with the Lewis acids B(C₆F₅)₃ and [CPh₃][B(C₆F₅)₄] afforded the desired ion pairs **3a,c** and **4b,c** (Scheme 2). **3c** was not soluble enough in benzene to allow detailed characterization and NMR studies. The solubility of **3a** was sufficient to obtain ¹H exchange spectroscopy (EXSY)^{27,28} NMR spectra but was too low for ¹⁹F/¹H heteronuclear Overhauser effect spectroscopy (HOESY)^{27,29} NMR experiments.

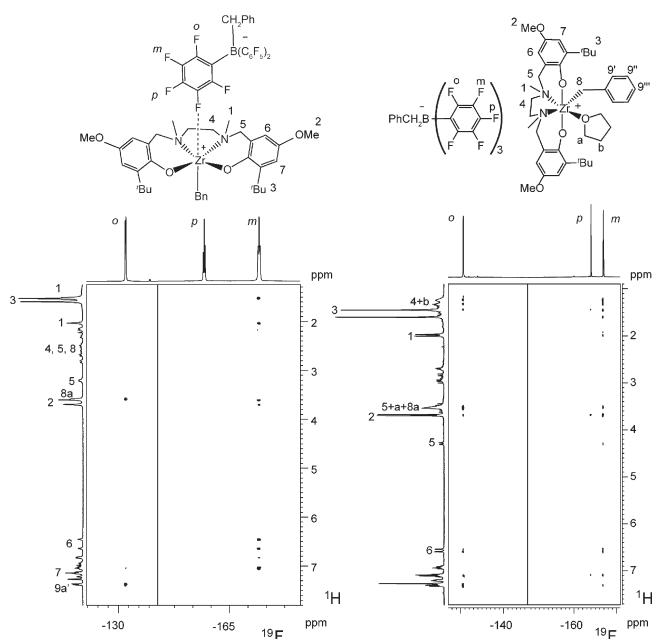


Figure 2. ^{19}F , ^1H -HOESY NMR spectra for **4b** (left) and **6b** (right) (C_6D_6 , 296 K).

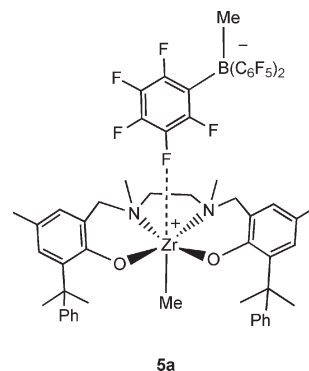
Table 1. Relevant ^1H and ^{19}F NMR Data (ppm) for Ion Pairs

	Zr-CH	B-CH	$ \Delta\delta(m,p-F) $
3a	0.61	1.47	2.74
3c	0.62		4.03
4b	2.68	3.59	2.99
6b	2.68	3.52	2.87
4c	2.66		4.01

Since olefin complexes of cations 3^+ and 4^+ are obviously unstable, we decided to use the THF complex of **4b** as a model for an olefin complex. Compound **4b** was reacted with an excess of dry tetrahydrofuran to generate the ion pair **6b** (Figure 2, right). The coordination of one molecule of THF is clear from the $-\text{OCH}_2-$ ^{13}C chemical shift value ($\delta_{\text{C}} \sim 76.5$ ppm), which is about 9 ppm higher than that of free THF in benzene,³⁰ and from integration of the respective ^1H NMR resonances.

Table 1 shows some relevant ^1H and ^{19}F NMR data for the ion pairs, indicating that in all cases the direct product of the activation is an OSIP, even in presence of the coordinating $\text{MeB}(\text{C}_6\text{F}_5)_3^-$ anion. In fact, the ^1H NMR resonance of the methyl bound to the boron falls at a rather high frequency value (δ_{H} 1.47 ppm) for **3a**, suggesting that it does not interact with the zirconium.^{31,32} As a confirmation, the difference in the ^{19}F chemical shift values between *m*-F and *p*-F resonances of the anion ($|\Delta\delta(m,p-F)|$) is 2.74 ppm, which is smaller than the literature value for having the anion in the first coordination sphere (usually 4.0–4.5 ppm).^{30,31} Complexes **4b** and **6b**, with the $\text{BnB}(\text{C}_6\text{F}_5)_3^-$ anion, which is generally considered less coordinating than $\text{MeB}(\text{C}_6\text{F}_5)_3^-$, show essentially the same $|\Delta\delta(m,p-F)|$ value (Table 1). In this case, it can be also noted that the interionic NOEs in the ^{19}F , ^1H -HOESY NMR spectrum are higher for *m*-F/H than for *o*-F/H (Figure 2), strengthening the hypothesis that the anion is in the second coordination sphere. Since the $\text{B}(\text{C}_6\text{F}_5)_4^-$ anion is even less coordinating than

Scheme 3. Geometry of Ion Pair **5a**



$\text{BnB}(\text{C}_6\text{F}_5)_3^-$,³³ it can be safely assumed that it too remains in the second coordination sphere.

The fact that even a rather “sticky” anion such as $\text{MeB}(\text{C}_6\text{F}_5)_3^-$ does not interact with the metal is an indication that the coordination vacancy is probably protected, either sterically or electronically.³⁴ In a recent communication¹⁶ we reported the first solution-phase characterization of a related complex (**5a**, Scheme 3): also in that case the methyl borate was in the second coordination sphere. Furthermore, the ^1H -NOESY experiments showed that the halves of the ligand were in slow chemical exchange and the anion showed the strongest contacts with the *N*Me group of one ligand half and the NCH_2Ar group of the other ligand half. This is incompatible with the *fac-fac* geometry and is in agreement with the *mer-mer* geometry. DFT calculations confirmed that the latter is the most stable geometry.¹⁶

For ion pair **4b**, in contrast to **5a**, exchange between the halves of the ligand is fast on the relaxation time scale, though slow on the chemical shift NMR time scale. As a consequence, the left and right halves of the ligand give rise to separate NMR signals, but in the ^{19}F , ^1H -HOESY NMR spectrum the NOE contacts between the anion and the ligand halves have the same intensities. However, the pattern of NOE cross-peaks for **4b** is similar to that reported for **5a**,¹⁶ with strong contacts between the *m*-F of the anion and protons of the *N*-methyl, the methoxy group, and one of the aromatic protons (1, 2, and 6, Figure 2). This fact and DFT calculations (see Computational Studies) confirm that also **4b** adopts the *mer-mer* geometry in solution. The absence of NOE contacts between the benzyl group of the anion and any proton of the cation indicates that the anion orients the fluorinated rings toward the cation, as was observed for $\text{MeB}(\text{C}_6\text{F}_5)_3^-$.^{31a,35,36}

For **6b** the situation is different. The left and right halves of the ligand are inequivalent and do not interconvert even on the relaxation time scale. The anion interacts not only with the protons mentioned above but also with the protons of the coordinated THF and the *tert*-butyl and benzyl groups (a, b, 3, and 9, Figure 2). This is only possible if the anion moves around, having different contact orientations of very similar stability. It seems that the anion has just a slight preference for staying close to the ethylenic bridge of the ligand (the normalized cross-peak³⁷ with the *tert*-butyl group is roughly half of that with the *N*-Me group). Unfortunately, many resonances overlap, making the exact quantification of the signal difficult. The analysis of the intramolecular NOE contacts does not yield any additional information about the ligand arrangement around the metal. The fact that there is no clearly preferred relative anion–cation orientation is probably due to the absence of any coordination vacancy in **6b**. Because of

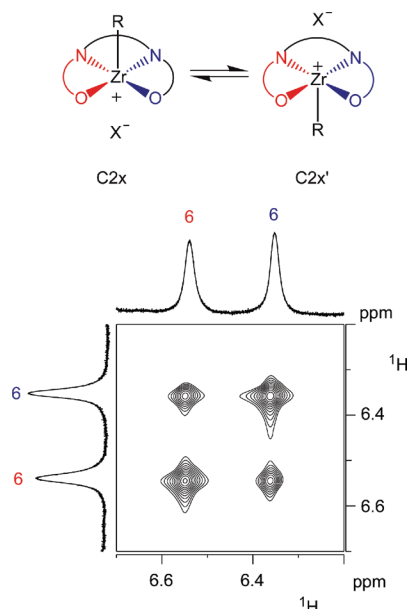


Figure 3. C2x–C2x' exchange process (top) and section of the ^1H -EXSY spectrum of **4b** (bottom) (benzene- d_6 , $T = 293$ K, mixing time 100 ms).

Table 2. Rate Constants of the Exchange Process Measured through ^1H -EXSY NMR Data (Benzene- d_6 , $\epsilon_{20^\circ\text{C}} = 2.28$)

entry	T (K)	k_i (s^{-1})
Compound 3a		
1	295.9	0.51
2	306.0	1.3
3	313.6	3.9
4	320.6	7.7
5 ^a	295.9	0.47
6 ^b	295.9	0.53
Compound 4b		
7	293.9	6.8
8	307.2	24.4
9	313.6	30.3
10	320.6	66.8
11	328.3	94.8
Compound 4c		
12	282.9	2.1
13	296.0	5.6
14	309.8	23.4

^a In the presence of an excess of $\text{B}(\text{C}_6\text{F}_5)_3$. ^b In $\text{C}_6\text{D}_5\text{Cl}$ ($\epsilon_{20^\circ\text{C}} = 5.6$).

Table 3. Activation Parameters (from Eyring Plots) for the C2x–C2x' Exchange Process^a

	ΔH_i^\ddagger	ΔS_i^\ddagger	r^2
3a	21 ± 1	-5 ± 2	0.986
4b	14 ± 1	-2 ± 2	0.958
4c	15 ± 1	-1 ± 3	0.941

^a ΔH_i^\ddagger is given in kcal/mol and ΔS_i^\ddagger in cal/(mol K); r^2 is the correlation coefficient.

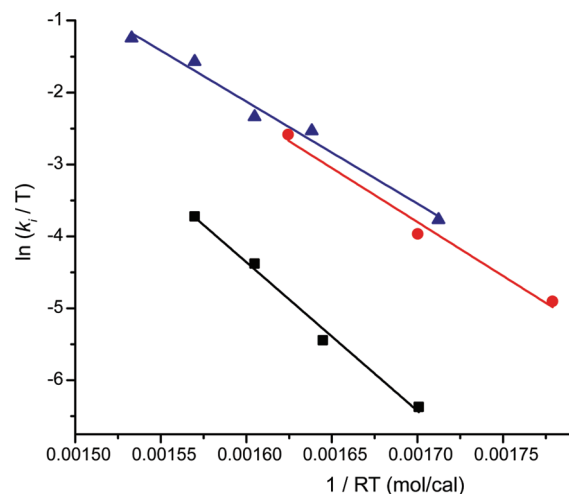


Figure 4. Eyring plots for the exchange processes of **3a** (black squares, ■), **4b** (red circles, ●), and **4c** (blue triangles, ▲). Solid lines represent the best linear fits.

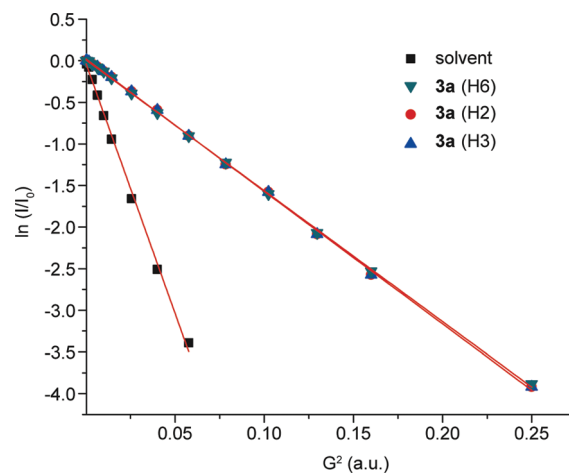


Figure 5. Plot of $\ln(I/I_0)$ versus G^2 for **3a** in benzene- d_6 ($c = 1$ mM).

this, it is not easy to unambiguously determine the conformation of the complex as was done for **5a**.¹⁶

^1H -EXSY Studies. All resonances in the ^1H NMR spectra of **3a** and **4b,c** (but not **6b**) are broadened due to a process that exchanges the analogous protons of the halves of the ligand (Figure 3).¹⁶ A series of ^1H -EXSY NMR spectra were recorded at different temperatures in order to determine the rate constant of the process (k_i) as a function of temperature and to extract the activation parameters for the C2x–C2x' exchange process of the different ion pairs. The results are collected in Tables 2 and 3. The rate of the exchange process is 0.51 s^{-1} for **3a** at 296 K (entry 1, Table 2), about half of that found previously for **5a** (1.2 s^{-1}).¹⁶ Both the addition of an excess of $\text{B}(\text{C}_6\text{F}_5)_3$ (entry 5, Table 2) and the use of a more polar solvent ($\text{C}_6\text{D}_5\text{Cl}$, entry 6, Table 2) have very little effect on k_i .

The activation parameters of the exchange process (Table 3) were determined from Eyring plots (Figure 4). ΔH_i^\ddagger is considerably higher for **3a** (21 kcal/mol) than for **4b,c** (14 and 15 kcal/mol, respectively), while ΔS_i^\ddagger is close to zero for all ion pairs.

PGSE NMR Studies. Pulsed-field gradient spin echo (PGSE) NMR experiments^{27,38} ($T = 295.6$ K, concentration around

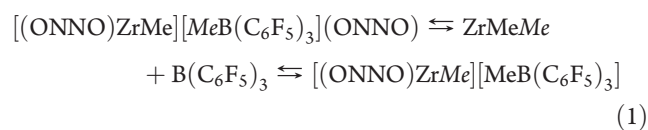
Table 4. Free Energy Differences (ΔG , kcal/mol) of Different Isomers

	C2x	C1	C2	C2_ISIP
Gas Phase (273 K, 1 bar)				
8 ⁺	0.0	−5.1	−9.38	
3a	0.0	1.4	18.1	6.2
4a	0.0	4.0	13.4	
7a	0.0	0.44	12.9	
Values Determined with COSMO ($\epsilon = 2.37$)				
3a	0.0	2.0	18.0	7.1
4a	0.0	5.2	13.9	
7a	0.0	1.1	12.8	

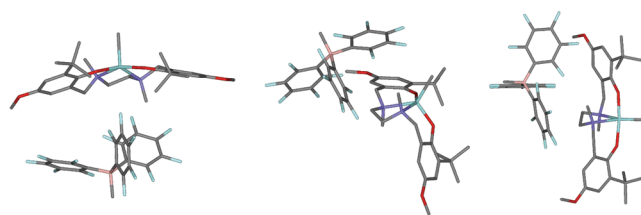
1 mM, Figure 5) were performed for **3a** in order to evaluate the average level of aggregation in solution. Since in all ion pairs the anion resides in the second coordination sphere, measurements were performed only for **3a** (MeB(C₆F₅)₃[−] counterion). OSIPs with various RB(C₆F₅)₃[−] counterions (R = alkyl, aryl) are known to have very similar tendencies to self-aggregate.^{35b} A self-diffusion coefficient of $4.55 \times 10^{-10} \text{ m}^2 \text{ s}^{-1}$ (calculated using the solvent residue as an internal reference)³⁹ was obtained from PGSE measurements.⁴⁰ Introducing this value in a modified version of the Stokes–Einstein equation³⁸ leads to a hydrodynamic volume of $1134 \pm 100 \text{ \AA}^3$ that is equal, within experimental error, to the volume of the ion pair in benzene, as evaluated from the DFT optimized geometry (1126 \AA^3).

Mechanism of the Exchange Process. Some conclusions can be drawn from the NMR studies about the mechanism of the exchange process:

- (i) The absence of the said process in **6b** indicates that a coordination vacancy plays a crucial role in the mechanism.
- (ii) The insensitivity of k_i to an excess of B(C₆F₅)₃ and to solvent polarity and the absence of any exchange peak between the methyl groups bound to zirconium and to boron rule out a methyl group transfer mechanism (eq 1).⁴¹



- (iii) Since the same k_i values are obtained in benzene and chlorobenzene, and the same trends of k_i versus $1/T$ are observed for **4b,c** (Figure 4), it can be concluded that the process does not depend on the anion. This is consistent with the fact that all the complexes are OSIPs in solution, as deduced from NMR studies.
- (iv) ΔS_i^\ddagger is rather small for all compounds studied, and only ion pairs are present in solution, as evidenced by the PGSE measurements, indicating that neither ion pair association (to ion quadruples) nor ion pair dissociation is likely to be involved.
- (v) Since the anion does not play a significant role, the difference in ΔH_i^\ddagger values between complexes containing 3⁺ and 4⁺ has to be attributed to the different alkyl groups bound to the zirconium. In particular, it seems that the transition state for the exchange process is lower in energy in the case of the benzyl group. The most likely explanation for such an effect is the ability of the benzyl group to adopt a η^2

**Figure 6.** Optimized structure of **3a_C2x** (left), **3a_C1** (center), and **3a_C2** (right). All hydrogens are omitted for clarity.

or η^3 coordination during the exchange process, provided it is cis to a coordination vacancy.⁴² This implies that the transition state should be closer to a *fac-mer* or *fac-fac* geometry than to the *mer-mer* arrangement.

Computational Studies. DFT calculations were carried out for cations 3⁺ and 4⁺ in combination with the MeB(C₆F₅)₃[−] counterion. This counterion was explicitly included for two reasons. (a) The difference in productivity between MAO/TBP and borate catalysts shows that the counterion affects the behavior of the catalyst somewhat. Presumably, having some kind of counterion is better than none at all. (b) All NMR studies were done with borate counterions; therefore, the NOE results can be directly correlated with the calculated structures. Since the counterions MeB(C₆F₅)₃[−], BnB(C₆F₅)₃[−], and B(C₆F₅)₄[−] behave so similarly both in NMR and in catalysis, we chose MeB(C₆F₅)₃[−] throughout for simplicity and computational efficiency. Species 7⁺, having an isobutyl group at Zr, was chosen to simulate the catalyst during polymerization.⁴³

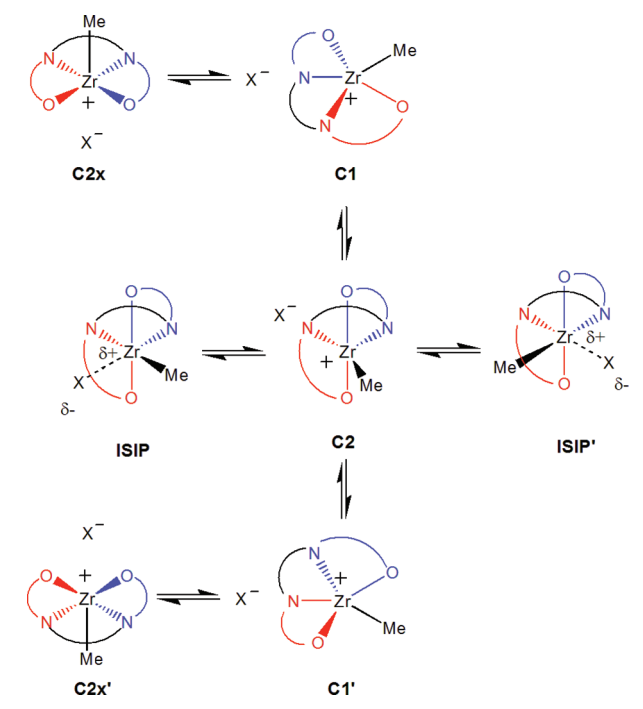
The energies of all the isomers depicted in Scheme 1 were calculated in order to evaluate their relative stability in solution and possibly locate the transition state of the C2x–C2x′ exchange process. In the presence of a coordinated dimethyl ether (8⁺), C2 is the most stable isomer, but if a coordination vacancy is present, C2x is the preferred species (Table 4),¹⁶ even relative to the C2-ISIP (ISIP = inner sphere ion pair), in good agreement with the experimental findings. Also, the dynamic behavior of these complexes is supported, the other isomers being not much higher in energy.

Considering the experimental results reported above, it can be assumed that the C2x–C2x′ exchange mechanism involves only movements of the O arms and the alkyl group. The anion, being already in the second coordination sphere, can easily “follow” the modification of the cation without playing an active role, as suggested by EXSY NMR data. **3a_C1** (Figure 6) can be considered as an intermediate species of the process. In fact, the Gibbs free energy of **3a_C1** is slightly higher than that of **3a_C2x** (Table 4), but its geometry is very different: it can be seen as a distorted-trigonal-bipyramidal complex (*fac-mer*), with an O arm and one of the nitrogen atoms occupying the apical positions (Figure 6).

3a_C1 can be easily formed from **3a_C2x** by just moving at the same time the methyl and one of the O arms from their initial positions in **3a_C2x** (axial and equatorial, respectively) to those shown in **3a_C1** (equatorial and axial, respectively), through “Berry pseudo-rotation” like movements⁴⁴ (Scheme 4). At the same time the anion shifts toward the least sterically hindered side of the complex, near the Zr–Me group.

Successively, the other O arm moves from the equatorial to the axial position, and the structure becomes **3a_C2**, a *fac-fac* trigonal-bipyramidal complex with both O arms in apical positions (Figure 6 and Scheme 4). From here, the methyl can move either right or left, creating a coordination vacancy that can trigger the

Scheme 4. Proposed Mechanism for the C2x–C2x' Exchange Process



exchange to **3a_C2x'** or back to **3a_C2x**. Alternatively, the vacancy can be filled, in principle at least, by the “sticky” MeB(C₆F₅)₃[−] anion (**3a_ISIP**, Scheme 4). All efforts to locate transition states for these steps failed: the potential energy surface appears to be too flat to allow a successful TS search.

It cannot be excluded that **3a_ISIP** is involved in the exchange process pathway, since its energy is lower than that of **3a_C2**. However, since its energy is higher than that of resting state **C2x**, its possible involvement in the sequence is kinetically irrelevant. This agrees with our observation that catalyst productivity does not depend on the nature of the borate counterion.

Although the transition state of the process has not been calculated, it can be noted that the energy of **3a_C2** (18 kcal/mol above **3a_C2x**) is just slightly lower than the experimental ΔG_1^\ddagger (21 kcal/mol). Assuming that DFT results can be directly compared with the experimental NMR data, this leads us to conclude that the **C2** → **C1** barrier is not very high. In other words, the transition state is probably very similar to **C2** in geometry and close to it in energy.

For the benzyl cation **4⁺**, the energy difference of **4a_C2** and **4a_C2x** was calculated to be “only” 13 kcal/mol due to the stabilization of **4a_C2** by η^3 coordination of the Zr-bound benzyl group (see the Supporting Information).⁴⁵ Consistent with this, also the observed ΔG_1^\ddagger value (from NMR) is reduced relative to the methyl analogue (to about 15 kcal/mol). Again, the **C2** → **C1** barrier is probably not very high.

Similarly to the benzyl group, the isobutyl chain is able to stabilize the **C2** structure, in this case by a β -agostic interaction⁴⁶ (CH–Zr distance equal to 2.21 Å): the calculated **7a_C2**/**7a_C2x** free energy difference is 13 kcal/mol. The energy cost of the isomerization from the “inactive” **C2x** ion pair to the “active” **C2** pair and the unfavorable polymerization activation entropy known for this class of catalysts¹⁸ seem to offer a rationale for their low productivity in polymerization.

It is important to outline that, although the counterion does not directly intervene in the pathway of the exchange process, its inclusion in the calculations seems to be crucial to reproduce the experimental activation parameters well. Particularly, the calculated energy difference of **4a_C2** and **4a_C2x** considering the naked cation is 6 kcal/mol, in strident disagreement with the experimental ΔG_1^\ddagger of 15 kcal/mol. It seems that the counterion plays a thermodynamic role in stabilizing the species involved in the **C2x**–**C2** isomerization process. This view could offer a rationale to the increase of activity observed with MAO that could be due to a destabilization of the **C2x** isomer (rather than to an improbable stabilization of the **C2** isomer).

CONCLUSIONS

The structure and dynamics in solution of some [bis(phenoxy-amine)ZrR]X ion pairs have been studied by means of NMR techniques and DFT calculations, showing that the most stable isomer has the ligand occupying all the equatorial coordination sites (**C2x**, *mer-mer* arrangement). However, the ligand conformation is dynamic in solution and it rapidly equilibrates between **C2x** and the **C2** species, which has the ligand surrounding the metal in a *fac-fac* arrangement and is able to coordinate and polymerize olefins. Notably, it has been demonstrated that the anion is not involved in the isomerization process and is located in the second coordination sphere of the metal. This explains why essentially the same polymer productivity is obtained with all the tested boron-based anions.⁴⁷

C₂-symmetric metallocene ion pairs undergo an apparently similar dynamic process (back skip),⁴⁰ but in that case the anion is strongly involved in the mechanism, tuning its rate and activation parameters: the apparent kinetic rate constant is usually around 0.5–30 s^{−1} for ISIPs and around 0.0001 s^{−1} for OSIPs.⁴⁸ For the [ONNO] catalysts studied here, even though they are OSIPs, the rates are similar to those of metallocene ISIPs. This is due to the fact that the two processes are in reality rather different. For a metallocene complex, epimerization simply comprises a shift of the alkyl group from one coordination position to the other one (preceded by counterion dissociation for an ISIP). For [bis(phenoxy-amine)ZrR]⁺X[−] ion pairs, on the other hand, the process involves a drastic change in geometry of the coordinated [ONNO] ligand.

Although only a few ONNO complexes have been studied so far, the **C2x**–**C2** isomerization process occurs in all of them, and it seems likely this is a general phenomenon. It might be important for other [(OYYO)MR][X] catalysts as well. Our studies indicate that the performance of the catalysts depends critically on the relative stability of the “active” **C2** isomer relative to the “inactive” **C2x** isomer. Since the **C2x**–**C2** isomerization process could represent the bottleneck of the polymerization process, conformational studies such as those reported here should be very helpful in arriving at an understanding of the factors controlling the **C2x**–**C2** isomerization reaction and, consequently, the polymerization process.

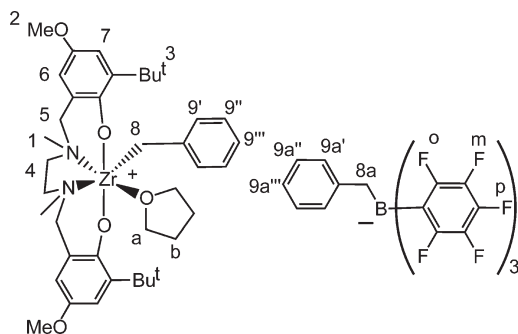
EXPERIMENTAL SECTION

All manipulations were performed in flamed Schlenk-type glassware interfaced to a high-vacuum line (<10^{−5} Torr) or in an argon-filled Braun LabMaster 130 glovebox (<1 ppm O₂). Molecular sieves (MS) were activated for 24 h at 200–230 °C under dynamic vacuum. All the solvents and liquid reagents were freeze–pump–thaw degassed on the high-vacuum line, dried over the appropriate drying agent, vacuum-transferred

to a dry storage tube with a PTFE valve, and stored over activated MS. Benzene- d_6 , toluene- d_8 , *n*-pentane, *n*-hexane, and toluene were dried over Na/K alloy. $B(C_6F_5)_3$ was obtained from Boulder Scientific Co. and was purified by sublimation (40–60 °C, 10^{-5} Torr). Toluene for polymerization runs (HPLC, Lab-Scan) was purified by passing it through a mixed-bed activated Cu/A4 molecular sieves column in an MBraun SPS-5 unit (final concentration of O_2 and H_2O <1 ppm). MAO (10% w/w solution in toluene) was purchased from Chemtura. 1H NMR analysis revealed it to contain 38% of Al as “free” $AlMe_3$. TBP was purchased from Aldrich. Propene (polymerization grade) was purchased from SON and used as received.

NMR samples were prepared in oven-dried J. Young NMR tubes. 1H , $^{13}C\{^1H\}$, 1H -COSY, 1H -NOESY/ 1H -EXSY, 1H -PGSE, 1H , ^{13}C -HMQC, 1H , ^{13}C -HMBC, ^{19}F , and ^{19}F , 1H -HOESY NMR experiments were performed on a Bruker Avance DRX 400 instrument equipped with a GREAT 1/10 gradient unit and a QNP probe with a Z-gradient coil, without spinning. Typical mixing times were 600 ms for the Overhauser experiments and within the range 4–600 ms for EXSY experiments. 1H -PGSE NMR data were treated as described in the literature.³⁸

Synthesis of [N,N'-Bis(3-*tert*-butyl-5-methoxy-2-hydroxyphenylmethyl)-N,N'-dimethylethylenediamine] (LigH₂). The ligand was prepared as described in the literature, but with minor changes.^{2a} A 441 mg portion of N,N'-dimethylethylenediamine (5 mmol), 749 μ L of formaldehyde solution (37 wt % in water, 10 mmol), and 1.8 g of 3-*tert*-butyl-4-hydroxyanisole (10 mmol) were dissolved in 15 mL of methanol and kept under reflux for 3 h. The precipitated product was filtered off, washed with cold methanol, and dried in an oven, at 65 °C under vacuum for 3 h. A second crop of product could be obtained by keeping the methanol solution in a refrigerator for several days. Total yields were ca. 85% (2.05 g). 1H NMR ($CDCl_3$, 295 K, 200 MHz, *J* in Hz): δ 10.4 (br, 2H, OH), 6.79 (d, 2H, $^4J_{H7,H6} = 3.00$, H7), 6.39 (d, 2H, H6), 3.74 (s, 6H, H2), 3.63 (s, 4H, H5), 2.60 (s, 4H, H4), 2.24 (s, 6H, H1), 1.38 (s, 18H, H3). $^{13}C\{^1H\}$ NMR ($CDCl_3$, 295 K, 50 MHz): δ 151.6 (–COCH₃), 150.5 (–COH), 137.9 (–CC(CH₃)₃), 122.2 (–CCH₂N), 112.7 (C6), 111.0 (C7), 62.5 (C5), 55.6 (C2), 53.5 (C4), 41.4 (C1), 34.8 (–C(CH₃)₃), 29.3 (C3). Anal. Calcd for $C_{28}H_{44}N_2O_4$: C, 71.15; H, 9.38; N, 5.93. Found: C, 71.40; H, 9.55; N, 5.82.



Synthesis of Complex 1. A 473 mg portion of LigH₂ (1 mmol) was dissolved in dry toluene (20 mL) and cooled to 0 °C. To this solution was added 1.3 mL of a *n*-BuLi solution (1.6 M in hexane, 2 mmol) dropwise, and the reaction mixture was warmed to room temperature. The resulting solution was added to a stirred suspension of 233 mg of $ZrCl_4$ (1 mmol) in dry toluene (10 mL) prepared previously. The reaction mixture was stirred at 80 °C for 2.5 h and then cooled to room temperature. To the resulting suspension was added 2.5 mL of MeMgBr solution (3.0 M in diethyl ether, 7.5 mmol), and the mixture was stirred overnight at room temperature.

The dark mixture was then evaporated under vacuum. To the residue was added fresh dry toluene (10 mL), and undissolved LiCl was removed by filtering the suspension through Celite that was washed

twice with dry toluene (2×5 mL). The combined filtrates were evaporated under vacuum, affording the product as a white solid, which was recrystallized from toluene/*n*-pentane and obtained in 85% final yield (502 mg). 1H NMR (C_6D_6 , 295 K, 400.13 MHz, *J* in Hz): δ 7.32 (d, 2H, $^4J = 2.94$, H7), 6.53 (d, 2H, $^4J = 2.94$, H6), 4.17 (d, 2H, $^2J = 13.31$, H5), 3.67 (s, 6H, H2), 2.72 (d, 2H, $^3J = 9.02$, H4), 2.52 (d, 2H, $^2J = 13.30$, H5), 1.87 (s, 24H, H3 + H1), 1.00 (d, 2H, $^3J = 9.20$, H4), 0.81 (s, 6H, Zr–CH₃). $^{13}C\{^1H\}$ NMR (C_6D_6 , 295 K, 100.55 MHz): δ 154.5, 152.5, 139.3, 126.0, 114.0 (C6), 113.9 (C7), 64.1 (C5), 55.7 (C2), 52.3 (C4), 45.6 (C1), 39.7 (Zr–CH₃), 35.7 (–C(CH₃)₃), 30.2 (C3). Anal. Calcd for $C_{30}H_{48}N_2O_4Zr$: C, 60.87; H, 8.17; N, 4.73. Found: C, 61.05; H, 8.38; N, 4.55.

Synthesis of Complex 2. The complex was synthesized as described in the literature, but with minor changes.^{2a} A 473 mg portion of LigH₂ (1 mmol) was weighed into a Schlenk flask and dissolved in dry toluene (10 mL). The resulting solution was added to another Schlenk flask containing a solution of Zr(benzyl)₄⁴⁹ (455 mg, 1 mmol) in the same solvent (10 mL). The mixture was kept at 65 °C for 2 h, and then the solvent was removed under vacuum to give the product as a pale yellow powder. Recrystallization from toluene/*n*-pentane afforded the product in 85% yield (630 mg). 1H NMR (C_6D_6 , 295 K, 400.13 MHz, *J* in Hz): δ 7.34 (d, 4H, $^3J = 7.21$, H9'), 7.26 (d, 2H, $^4J = 2.93$, H7), 7.21 (t, 4H, $^3J = 8.07$, H9''), 6.92 (t, 2H, $^3J = 7.41$, H9'''), 6.42 (d, 2H, $^4J = 2.93$, H6), 3.75 (d, 2H, $^2J = 13.41$, H5), 3.59 (s, 6H, H2), 2.99 (d, 2H, $^2J = 10.48$, H8), 2.66 (d, 2H, $^2J = 9.19$, H4), 2.55 (d, 2H, $^2J = 10.33$, H8), 2.37 (d, 2H, $^2J = 13.78$, H5), 1.86 (m, 24H, H3 and H1), 0.90 (d, 2H, $^4J = 9.49$, H7). $^{13}C\{^1H\}$ NMR (C_6D_6 , 295 K, 100.55 MHz): δ 153.4, 152.7, 148.9, 139.2, 128.8, 127.5, 127.2, 126.5, 121.6, 113.8 (C6), 113.5 (C7), 69.1 (C8), 64.0 (C5), 55.3 (C2), 52.8 (C4), 45.6 (C1), 35.8 (C(CH₃)₃), 30.5 (C3). Anal. Calcd for $C_{42}H_{56}N_2O_4Zr$: C, 67.79; H, 7.59; N, 3.76. Found: C, 67.95; H, 7.78; N, 3.53.

Synthesis of Ion Pair 3a. A 10 mg portion of complex 1 (17 μ mol) and 12 mg of $B(C_6F_5)_3$ (23 μ mol) were dissolved in dry toluene (0.5 mL). The solution became pale yellow, and a yellow oily phase separated. The latter was washed with dry pentane and dried under vacuum, affording the desired product as an oil that is poorly soluble in benzene. 1H NMR (C_6D_6 , 295 K, 400.13 MHz, *J* in Hz): δ 7.10 (d, 1H, $^4J = 2.58$, H7), 7.02 (d, 1H, $^4J = 2.69$, H7), 6.57 (d, 1H, $^4J = 2.60$, H6), 6.47 (d, 1H, $^4J = 2.34$, H7), 3.80 (d, 2H, $^2J = 14.28$, H5), 3.60 (s, 3H, H2), 3.54 (s, 3H, H2), 3.07 (d, 1H, $^2J = 14.74$, H5), 3.02 (d, 1H, $^2J = 14.65$, H5), 2.78 (m, 2H, H4), 2.33 (d, 1H, $^2J = 10.84$, H4), 2.03 (d, 1H, $^2J = 10.84$, H4), 1.89 (s, 3H, H1), 1.68 (s, 3H, H1), 1.47 (br s, 3H, B–Me), 1.32 (s, 9H, H3), 1.30 (s, 9H, H3), 0.61 (s, 3H, Zr–Me). ^{19}F NMR (C_6D_6 , 295 K, 376.65 MHz, *J* in Hz): δ –132.11 (br d, 6F, $^3J = 20.7$, *o*), –163.95 (t, 3F, $^3J = 20.7$, *p*), –166.69 (br t, 6F, $^3J = 19.4$, *m*). The solubility was too low to allow ^{13}C NMR measurements.

Synthesis of Ion Pair 3c. A 10 mg portion of complex 1 (17 μ mol) and 20 mg of $[C(C_6H_5)_3][B(C_6F_5)_4]$ (22 μ mol) were dissolved in dry toluene (0.5 mL). The solution became bright yellow, and a yellow oily phase separated. The latter was washed twice with dry toluene (about 0.8 mL) and dried under vacuum, affording the desired product as an oil that is poorly soluble in benzene ($<10^{-4}$ M). 1H NMR (C_6D_6 , 295 K, 400.13 MHz, *J* in Hz): δ 7.47 (br, 2H, H9a'), 7.35 (t, 3H, $^3J = 7.03$, H9a''), 7.04 (m, overlapped with solvent), 6.77 (d, 2H, $^3J = 7.50$, H9'), 6.56 (br s, 1H, H6), 6.53 (br s, 1H, H6), 3.62 (br s, 3H, H2), 3.60 (5H, H2 and H5), 2.97 (m, 3H, H8), 1.78 (s, 3H, H1), 1.55 (br s, 12H, H1 and H3), 1.49 (s, 9H, H3), 1.36 (m, H4), 0.62 (s, 3H, H8). ^{19}F NMR (C_6D_6 , 295 K, 376.65 MHz, *J* in Hz): δ –132.09 (m, 6F, *o*), –162.42 (t, 3F, $^3J = 21.1$, *p*), –166.45 (m, 6F, *m*). The solubility was too low to allow ^{13}C NMR measurements.

Synthesis of Ion Pair 4b. A 20 mg portion of complex 2 (27 μ mol) and 16 mg of $B(C_6F_5)_3$ (31 μ mol) were dissolved in dry toluene (0.5 mL). The resulting solution was stirred, and the solution became pale yellow. The addition of pentane led to the formation of a dark yellow

oily phase. The latter was separated, washed with dry pentane, and dried under vacuum, affording the desired product as an oil. ^1H NMR (C_6D_6 , 295 K, 400.13 MHz, J in Hz): δ 7.37 (d, 2H, $^3J = 7.29$, H9a'), 7.22 (s, 1H, H7), 7.14 (m, 3H, H9a'' and H7), 7.00 (m, 5H, H9a''', H9''' and H9''), 6.83 (d, 2H, $^3J = 7.09$, H9'), 6.64 (s, 1H, H6), 6.45 (s, 1H, H6), 3.7 (s, 3H, H2), 3.59 (m, 3H, H2 and H8a), 3.22 (d, 1H, $^2J = 12.17$, H5), 3.19 (d, 1H, $^2J = 12.17$, H5), 2.82 (d, 1H, $^2J = 14.56$, H5), 2.68 (d, 1H, $^2J = 11.72$, H8), 2.54 (m, 2H, H4 and H5), 2.30 (d, 1H, $^2J = 12.01$, H4), 2.16 (d, 2H, $^2J = 11.60$, H4), 2.03 (s, 3H, H1), 1.56 (s, 9H, H3), 1.53 (s, 9H, H3), 1.51 (s, 3H, H1). $^{13}\text{C}\{^1\text{H}\}$ NMR (C_6D_6 , 295 K, 100.55 MHz): δ 155.4, 151.9, 150.1, 148.1, 139.1, 137.7, 136.1, 131.1, 129.4, 129.0, 128.4, 128.1, 127.8, 126.8, 124.4, 123.6, 123.1, 116.3 (C6), 115.2 (C6), 112.9 (C7), 112.0 (C7), 72.7 (C8), 65.4 (C4), 62.2 (C5), 57.4 (C2), 55.2 (C2), 42.8 (C1), 38.2 (C1), 35.6 (2C, C(CH₃)₃), 30.3 (C3), 30.1 (C3). ^{19}F NMR (C_6D_6 , 295 K, 376.65 MHz, J in Hz): δ -130.71 (br d, 6F, $^3J = 22.6$, o), -163.63 (t, 3F, $^3J = 21.1$, m), -166.62 (br t, 6F, $^3J = 21.1$, p).

Synthesis of Ion Pair 4c. A 20 mg portion of **2** (27 μmol) and 28 mg of $[\text{C}(\text{C}_6\text{H}_5)_3][\text{B}(\text{C}_6\text{F}_5)_4]$ (31 μmol) were dissolved in dry toluene (0.5 mL). The resulting solution was stirred, and the solution became red. The addition of pentane led to the formation of a dark oily phase. The latter was separated, washed twice with dry toluene and once with pentane, and dried under vacuum, affording the desired product as an oil. ^1H NMR (C_6D_6 , 295 K, 400.13 MHz, J in Hz): δ 7.21 (s, 1H, H7), 7.14 (s, 1H, H7), 7.02 (t, 2H, $^3J = 7.40$, H9''), 6.92 (t, 1H, $^3J = 7.12$, H9'), 6.81 (d, 2H, $^3J = 7.20$, H9''). 6.61 (s, 1H, H6), 6.42 (s, 1H, H6), 3.66 (s, 3H, H2), 3.57 (m, 3H, H2), 3.22 (d, 1H, $^2J = 13.41$, H5), 3.14 (d, 1H, $^2J = 13.17$, H5), 2.79 (d, 1H, $^2J = 14.49$, H5), 2.66 (d, 1H, $^2J = 11.50$, H8), 2.55 (m, 2H, H4 and H5), 2.27 (d, 1H, $^2J = 14.22$, H4), 2.13 (m, 2H, H4), 2.03 (s, 3H, H1), 1.59 (s, 9H, H3), 1.52 (s, 9H, H3), 1.50 (s, 3H, H1). ^{19}F NMR (C_6D_6 , 295 K, 376.65 MHz, J in Hz): δ -132.13 (m, 6F, o), -162.31 (t, 3F, $^3J = 21.1$, p), -166.32 (m, 6F, m). The solubility was too low to allow ^{13}C NMR measurements.

Synthesis of Ion Pair 6b. A 15 mg portion of ion pair **4b** (12 μmol) was dissolved in dry toluene (0.5 mL) in the presence of an excess of dry tetrahydrofuran. After stirring, the solvent was removed by vacuum. The resulting solid was washed with pentane and dried under vacuum. ^1H NMR (C_6D_6 , 295 K, 400.13 MHz, J in Hz): δ 7.31 (m, 4H, H9' and H9a'), 7.21 (m, 2H, H7), 7.12 (t, 2H, $^3J = 7.66$, H9''), 7.08 (t, 2H, $^3J = 7.50$, H9a''), 6.93 (m, 2H, 9'' and 9a'''), 6.59 (d, 1H, $^4J = 2.73$, H6), 6.54 (d, 1H, $^4J = 2.78$, H6), 7.08 (t, 2H, $^3J = 7.50$, H9a''), 4.29 (d, 1H, $^2J = 14.19$, H5), 3.70 (s, 3H, H2), 3.67 (s, 3H, H2), 3.52 (m, 6H, H8a and Ha), 3.46 (d, 1H, $^2J = 14.19$, H5), 2.89 (m, 4H, H4, H5, and H8), 2.83 (d, 1H, $^2J = 14.93$, H5), 2.68 (m, 1H, H8), 2.00 (s, 3H, H1), 1.97 (s, 3H, H1), 1.60 (s, 9H, H3), 1.45 (s, 9H, H3), 1.28 (m, 5H, Hb and H4). $^{13}\text{C}\{^1\text{H}\}$ NMR (C_6D_6 , 295 K, 100.55 MHz): δ 154.7, 154.3, 150.8, 150.6, 149.2, 139.3, 136.2, 134.5, 133.1, 130.6, 129.8, 129.3, 128.8, 128.3, 127.7, 126.5, 126.1, 125.6, 123.4, 115.7 (C6), 115.0 (C6), 113.9 (C7), 113.2 (C7), 76.5 (THF, a), 64.0 (C4), 55.4 (2C, C2), 51.9 (C5), 47.3 (2C, C1), 35.4 (C(CH₃)₃), 35.3 (C(CH₃)₃), 30.5 (C3), 30.3 (C3), 25.6 (THF, b). ^{19}F NMR (C_6D_6 , 295 K, 376.65 MHz, J in Hz): δ -130.62 (br d, 6F, $^3J = 22.5$, o), -164.02 (t, 3F, $^3J = 21.0$, p), -166.89 (br t, 6F, $^3J = 20.6$, m).

Polymerization Runs. Polymerization experiments were carried out with a high-throughput parallel reactor setup (PPR24, available from Freeslate, Inc.) with three reactor modules, each containing eight reaction cells (6 mL working volume per cell). The whole system is housed in a triple MBraun LabMaster glovebox maintaining a pure nitrogen atmosphere (oxygen and water levels <1 ppm). The monomer gas and quench gas lines were plumbed directly into the reactors and controlled by automatic valves; propene was fed after purification by passing through columns containing a mixed bed of 4A molecular sieves (3.2 mm pellets) and an activated copper catalyst (BASF R 3-11G). Liquid reagents were robotically added to individual cells by syringes. Solvents were previously purified in an MBraun SPS unit.

For the purpose of this work, each reactor module was used to screen precatalysts **1** and **2** in combination with MAO, MAO/TBP, $[\text{CPh}_3][\text{B}(\text{C}_6\text{F}_5)_4]/\text{TIBA}$, and $\text{B}(\text{C}_6\text{F}_5)_3/\text{TIBA}$ (TIBA = triisobutylaluminum) according to the following procedure. The cells were fitted with a preweighed glass vial insert and a disposable stirring paddle. The reactor was closed, and then the scavenger was injected into each cell through a valve: 150 or 100 μL of a 0.020 M solution of MAO (MAO, Chemtura, 10% w/w solution in toluene) or TIBA (TIBA, Chemtura) in toluene (toluene HPLC, Lab-Scan, 99.8%) and 3.25 (or 4.15) mL of toluene. The reactor temperature was set to 60 $^\circ\text{C}$, and stirring was started at a speed of 800 rpm. The reactor was pressurized at 5.5 bar (80 psi) with propene.

In an array of 18 \times 1.2 mL glass vials positioned on a vortexer, precatalysts and activators were premixed immediately prior to addition into the cells (for activation with MAO and MAO/TBP, $[\text{Al}]/[\text{Zr}] = 100$ and $[\text{TBP}]/[\text{Al}] = 0.5$, for activation with $[\text{CPh}_3][\text{B}(\text{C}_6\text{F}_5)_4]/\text{TIBA}$, $[\text{B}]/[\text{Zr}] = 1.2$, for activation with $\text{B}(\text{C}_6\text{F}_5)_3/\text{TIBA}$, $[\text{B}]/[\text{Zr}] = 1.0$; in the last two cases, no further TIBA was used apart from that used as scavenger). Aliquots of the catalyst system solutions containing the desired amount of catalyst (typically 50–100 mg corresponding to a reaction time of 10–60 min) were then injected into the cells. The polymerization was run at constant temperature and propene partial pressure until the targeted propene uptake was reached, at which point the reaction was quenched with air at 3.4 bar (50 psi) overpressure. The reactor was opened, and the glass inserts were unloaded from the cells, transferred to a centrifuge/vacuum drying unit (Genevac EZ-2 Plus), and dried to constant weight, after which the polymer samples were recovered and weighed on a Bohdan BA-100 Balance Automator unit. The reproducibility of polymer yields on experiments in duplicate turned out to be better than +20%.

Computational Details. Density functional calculations were performed with the Turbomole program⁵⁰ (version 5.8) in combination with the OPTIMIZE routine of Baker and co-workers.⁵¹ All geometries were fully optimized at the restricted RI⁵²-BP86⁵³ level, using the SV(P)⁵⁴ basis set (small-core pseudopotential on Zr⁵⁵). For each structure the analytical frequencies were calculated, in order to check that no imaginary values were present. Thermal corrections (enthalpy and entropy) were calculated for the gas phase, 273 K, 1 bar, using the standard formulas of statistical thermodynamics.⁵⁶

Single-point solvent corrections were calculated using the conductor-like screening model (COSMO)⁵⁷ with $\epsilon = 2.37$ to model an apolar solvent (e.g., toluene). All energies mentioned in the text include this solvation correction, unless noted otherwise. Initial geometries and reasonable starting Hessians were obtained from PM3 computations with the Spartan package from Wavefunction Inc.⁵⁸

■ ASSOCIATED CONTENT

Supporting Information. Figures giving DFT-optimized structures of all the species considered. This material is available free of charge via the Internet at <http://pubs.acs.org>.

■ AUTHOR INFORMATION

Corresponding Author

*E-mail: alceo@unipg.it (A.M.); budzela@cc.umanitoba.ca (P.H.M.B.).

■ ACKNOWLEDGMENT

This work is part of the Research Programme of the Dutch Polymer Institute, Eindhoven, The Netherlands (project no. #633).

REFERENCES

- (1) (a) Gibson, V. C.; Spitzmesser, S. K. *Chem. Rev.* **2003**, *103* (1), 283. (b) Britovsek, G. J. P.; Gibson, V. C.; Wass, D. F. *Angew. Chem., Int. Ed.* **1999**, *38* (4), 428. (c) Busico, V. *Macromol. Chem. Phys.* **2007**, *208* (1), 26 and references therein. (d) Matsugi, T.; Fujita, T. *Chem. Soc. Rev.* **2008**, *37* (6), 1264. (e) Corradini, P.; Guerra, G.; Cavallo, L. *Acc. Chem. Res.* **2004**, *37* (4), 231. (f) Coates, G. W. *Chem. Rev.* **2000**, *100* (4), 1223. (g) Lamberti, M.; Mazzeo, M.; Pappalardo, D.; Pellicchia, C. *Coord. Chem. Rev.* **2009**, *253*, 2082.
- (2) (a) Tshuva, E. T.; Goldberg, I.; Kol, M. *J. Am. Chem. Soc.* **2000**, *122* (43), 10706. (b) Gendler, S.; Zelikoff, A. L.; Kopilov, J.; Goldberg, I.; Kol, M. *J. Am. Chem. Soc.* **2008**, *130* (7), 2144. (c) Meppelder, G.-J.; Fan, H.-T.; Spaniol, T. P.; Okuda, J. *Organometallics* **2009**, *28* (17), 5159.
- (3) Long, R. J.; Jones, D. J.; Gibson, V. C.; White, A. J. P. *Organometallics* **2008**, *27* (22), 5960.
- (4) (a) Cohen, A.; Yeori, A.; Goldberg, I.; Kol, M. *Inorg. Chem.* **2007**, *46* (20), 8114. (b) Ishii, A.; Toda, T.; Nakata, N.; Matsuo, M. *J. Am. Chem. Soc.* **2001**, *131* (38), 13566.
- (5) Boussie, T. R.; Brummer, O.; Diamond, G. M.; Goh, C.; Lapointe, A. M.; Leclerc, M. K.; Shoemaker, J. A. (Symyx Technologies, Inc.) WO 03/091262 A1, 2003.
- (6) (a) Moore, E. P., Jr., Ed. *Polypropylene Handbook: Polymerization, Characterization, Properties, Applications*; Hanser: Munich, 1996. (b) Boor, J., Jr. *Ziegler–Natta Catalysts and Polymerizations*; Academic: New York, 1979.
- (7) Busico, V.; Cipullo, R.; Pellicchia, R.; Ronca, S.; Roviello, G.; Talarico, G. *Proc. Natl. Acad. Sci. U.S.A.* **2006**, *103* (42), 15321.
- (8) (a) Segal, S.; Goldberg, I.; Kol, M. *Organometallics* **2005**, *24* (2), 200. (b) Yeori, A.; Groysman, S.; Goldberg, I.; Kol, M. *Inorg. Chem.* **2005**, *44* (13), 4466. (c) Yeori, A.; Gendler, S.; Groysman, S.; Goldberg, I.; Kol, M. *Inorg. Chem. Commun.* **2004**, *7* (2), 280.
- (9) (a) Busico, V.; Cipullo, R.; Ronca, S.; Budzelaar, P. H. M. *Macromol. Rapid Commun.* **2001**, *22* (17), 1405. (b) Busico, V.; Cipullo, R.; Friederichs, N.; Ronca, S.; Talarico, G.; Togrou, M.; Wang, B. *Macromolecules* **2004**, *37* (22), 8201.
- (10) (a) Cohen, A.; Kopilov, J.; Goldberg, I.; Kol, M. *Organometallics* **2009**, *28* (5), 1391. (b) Zelikoff, A. L.; Kopilov, J.; Goldberg, I.; Coates, G. W.; Kol, M. *Chem. Commun.* **2009**, 6804.
- (11) (a) Hormnirun, P.; Marshall, E. L.; Gibson, V. C.; White, A. J. P.; Williams, D. J. *J. Am. Chem. Soc.* **2004**, *126* (9), 2688. (b) Du, H.; Velders, A. H.; Dijkstra, P. J.; Sun, J.; Zhong, Z.; Chen, X.; Feijen, J. *Chem. Eur. J.* **2009**, *15* (38), 9836.
- (12) Darensbourg, D. J.; Ulusoy, M.; Karroonnirum, O.; Poland, R. R.; Reibenspies, J. H.; Çetinkaya, B. *Macromolecules* **2009**, *42* (18), 6992.
- (13) Salavati-Niasari, M.; Shakouri-Arani, M.; Davar, F. *Microporous Mesoporous Mater.* **2008**, *116* (1), 77.
- (14) Flisak, Z.; Suchorska, P. *Organometallics* **2010**, *29* (23), 6196.
- (15) Unpublished results from Macchioni's laboratory.
- (16) Ciancaleoni, G.; Fraldi, N.; Budzelaar, P. H. M.; Busico, V.; Macchioni, A. *Dalton Trans.* **2009**, *41*, 8824.
- (17) Macchioni, A. *Chem. Rev.* **2005**, *105*, 2039.
- (18) Actually the indicated symmetries refer to the neutral catalyst precursors, but it is common usage to associate them also to the derived ion pairs.
- (19) Ciancaleoni, G.; Fraldi, N.; Budzelaar, P. H. M.; Busico, V.; Cipullo, R.; Macchioni, A. *J. Am. Chem. Soc.* **2010**, *132* (39), 13651.
- (20) (a) Andresen, A.; Cordes, H. G.; Herwig, H.; Kaminsky, W.; Merk, A.; Mottweiler, R.; Pein, J.; Sinn, H.; Vollmer, H. J. *Angew. Chem., Int. Ed. Engl.* **1976**, *15* (10), 630. (b) Sinn, H.; Kaminsky, W.; Vollmer, H. J.; Woldt, R. *Angew. Chem., Int. Ed. Engl.* **1980**, *19* (5), 390.
- (21) Experimental works: (a) Talsi, E. P.; Semikolenova, N. V.; Panchenko, V. N.; Sobolev, A. P.; Babushkin, D. E.; Shubin, A. A.; Zakharov, V. A. *J. Mol. Catal. A: Chem.* **1999**, *139* (2), 131. (b) Babushkin, D. E.; Brintzinger, H. H. *J. Am. Chem. Soc.* **2002**, *124* (43), 12869. (c) Stellbrink, J.; Niu, A.; Allgaier, J.; Richter, D.; Koenig, B. W.; Hartmann, R.; Coates, G. W.; Fetters, L. J. *Macromolecules* **2007**, *40* (14), 4972. Theoretical works: (d) Zakharov, I. I.; Zacharov, V. A. *Macromol. Theory Simul.* **2002**, *11* (3), 352. (e) Negureanu, L.; Hall, R. W.; Butler, L. G.; Simeral, L. A. *J. Am. Chem. Soc.* **2006**, *128* (51), 16816. (f) Zurek, E.; Woo, T. K.; Firman, T. K.; Ziegler, T. *Inorg. Chem.* **2001**, *40* (2), 361.
- (22) Zurek, E.; Ziegler, T. *Prog. Polym. Sci.* **2004**, *29* (2), 107 and references therein.
- (23) (a) Busico, V.; Cipullo, R.; Cutillo, F.; Friederichs, N.; Ronca, S.; Wang, B. *J. Am. Chem. Soc.* **2003**, *125* (41), 12402. (b) Rouhollahnejad, F.; Mathis, D.; Chen, P. *Organometallics* **2010**, *29* (2), 294.
- (24) (a) Zhou, J.; Lancaster, S. J.; Walker, D. A.; Beck, S.; Thornton-Pett, M.; Bochmann, M. *J. Am. Chem. Soc.* **2001**, *123* (2), 223. (b) Wilson, P. A.; Hannant, M. H.; Wright, J. A.; Cannon, R. D.; Bochmann, M. *Macromol. Symp.* **2006**, *236* (1), 100.
- (25) Bochmann, M. *Organometallics* **2010**, *29* (21), 4711.
- (26) Chen, E. Y.-X.; Marks, T. J. *Chem. Rev.* **2000**, *100* (4), 1391.
- (27) Perrin, C. L.; Dwyer, T. J. *Chem. Rev.* **1990**, *90* (6), 935.
- (28) Ciancaleoni, G.; Zuccaccia, C.; Zuccaccia, D.; Macchioni, A. *Techniques in Inorganic Chemistry*; Fackler, J. P., Jr., Falvello, L., Eds.; CRC Press Taylor & Francis Group: Boca Raton, FL, 2010; pp 129–180.
- (29) (a) Macchioni, A. *Eur. J. Inorg. Chem.* **2003**, 195. (b) Bellachioma, G.; Cardaci, G.; Gramlich, V.; Macchioni, A.; Valentini, M.; Zuccaccia, C. *Organometallics* **1998**, *17*, 5025. (c) Bellachioma, G.; Ciancaleoni, G.; Zuccaccia, C.; Zuccaccia, D.; Macchioni, A. *Coord. Chem. Rev.* **2008**, *252* (21), 2224. (d) Pregoni, P. S.; Kumar, P. G. A.; Fernandez, I. *Chem. Rev.* **2005**, *105* (8), 2977.
- (30) Gottlieb, H. E.; Kotlyar, V.; Nudelman, A. *J. Org. Chem.* **1997**, *62* (21), 7512.
- (31) See for comparison ref 31 and: (a) Horton, A. D.; de With, J. *Organometallics* **1997**, *16* (25), 5424. (b) Horton, A. D.; de With, J. *Chem. Commun.* **1996**, *11*, 1375. (c) Horton, A. D.; de With, J.; van der Linden, A. J.; van de Weg, H. *Organometallics* **1996**, *15* (12), 2672.
- (32) (a) Schaper, F.; Geyer, A.; Britzinger, H. H. *Organometallics* **2002**, *21* (3), 473. (b) Zuccaccia, C.; Stahl, N. G.; Macchioni, A.; Chen, M.-C.; Roberts, J. A.; Marks, T. J. *J. Am. Chem. Soc.* **2004**, *126* (5), 1448. (c) Song, F.; Lancaster, S. J.; Cannon, R. D.; Schormann, M.; Humphrey, S. M.; Zuccaccia, C.; Macchioni, A.; Bochmann, M. *Organometallics* **2005**, *24* (6), 1315. (d) Zuccaccia, C.; Busico, V.; Cipullo, R.; Talarico, G.; Froese, R. D. J.; Vosejka, P. C.; Hustad, P. D.; Macchioni, A. *Organometallics* **2009**, *28* (18), 5445.
- (33) Jia, L.; Yang, X.; Stern, C. L.; Marks, T. J. *Organometallics* **1997**, *16* (5), 842.
- (34) Stapleton, R. A.; Galan, B. R.; Collins, S.; Simons, R. S.; Garrison, J. C.; Youngs, W. J. *J. Am. Chem. Soc.* **2003**, *125* (31), 9246.
- (35) (a) Zuccaccia, C.; Bellachioma, G.; Cardaci, G.; Macchioni, A. *J. Am. Chem. Soc.* **2001**, *123* (44), 11020. (b) Rocchigiani, L.; Bellachioma, G.; Ciancaleoni, G.; Macchioni, A.; Zuccaccia, D.; Zuccaccia, C. *Organometallics* **2011**, *30* (1), 100.
- (36) Correa, A.; Cavallo, L. *J. Am. Chem. Soc.* **2006**, *128* (33), 10952.
- (37) The volumes of the peaks were normalized for the number of equivalent protons through the parameter $f = [n_1 n_5 / (n_1 + n_5)]$ (n_1 = number of equivalent nuclei of the first type, n_5 = number of equivalent nuclei of the second type); see: Macura, S.; Ernst, R. R. *Mol. Phys.* **1980**, *41*, 95.
- (38) (a) Hahn, E. L. *Phys. Rev.* **1950**, *80* (4), 580. (b) Stejskal, E. O.; Tanner, J. E. *J. Chem. Phys.* **1965**, *42* (1), 288. (c) Stilbs, P. *Prog. Nucl. Magn. Reson. Spectrosc.* **1987**, *19* (1), 1. (d) Price, W. S. *Conc. Magn. Reson.* **1997**, *9*, 299. (e) Price, W. S. *Conc. Magn. Reson.* **1998**, *10*, 197.
- (39) Macchioni, A.; Ciancaleoni, G.; Zuccaccia, C.; Zuccaccia, D. *Chem. Soc. Rev.* **2008**, *37* (3), 479.
- (40) This self-diffusion coefficient was obtained following the resonances of the cation; since the solvent is nonpolar, only even aggregates, as ion pairs and quadruples, are likely present: Rocchigiani, L.; Bellachioma, G.; Ciancaleoni, G.; Crocchianti, S.; Laganà, A.; Zuccaccia, C.; Zuccaccia, D.; Macchioni, A. *Chem. Phys. Chem.* **2010**, *11* (15), 3243.
- (41) (a) Beswick, C. L.; Marks, T. J. *J. Am. Chem. Soc.* **2000**, *122* (42), 10358. (b) Deck, P. A.; Beswick, C. L.; Marks, T. J. *J. Am. Chem. Soc.* **1998**, *120* (8), 1772. (c) Deck, P. A.; Marks, T. J. *J. Am. Chem. Soc.* **1995**, *117* (22), 6128. (d) Chen, Y.-X.; Yang, S.; Stern, C. L.; Marks, T. J.

J. Am. Chem. Soc. **1996**, *118* (49), 12451. (e) Yang, X.; Stern, C. L.; Marks, T. J. *J. Am. Chem. Soc.* **1994**, *116* (22), 10015.

(42) (a) Tsukahara, T.; Swenson, D. C.; Jordan, R. F. *Organometallics* **1997**, *16* (15), 3303. (b) Lee, H.; Jordan, R. F. *J. Am. Chem. Soc.* **2005**, *127* (26), 9384. (c) Girolami, G. S.; Wilkinson, G.; Thornton-Pett, M.; Hursthouse, M. B. *J. Chem. Soc., Dalton Trans.* **1984**, *12*, 2789. (d) Ong, T. G.; Wood, D.; Yap, G. P. A.; Richeson, D. S. *Organometallics* **2002**, *21* (1), 1.

(43) Ducère, J.-M.; Cavallo, L. *Organometallics* **2006**, *25* (6), 1431.

(44) (a) Berry, R. S. *J. Chem. Phys.* **1960**, *32*, 933. (b) Dunitz, J. D.; Prelog, V. *Angew. Chem.* **1968**, *80*, 700. (c) Montgomery, C. D. *J. Chem. Educ.* **2001**, *78* (6), 844. (d) <http://www.ch.ic.ac.uk/rzepa/bpr>.

(45) Zr–CH₂ = 2.35 Å, Zr–C_{ipso} = 2.61 Å, Zr–C_{ortho} = 2.66 Å, Zr–CH₂–C_{ipso} = 82.9°. See for comparison ref 41.

(46) Woo, T. K.; Fan, L.; Ziegler, T. *Organometallics* **1994**, *13* (6), 2252.

(47) Only the use of MAO/TBP as cocatalyst leads to a somewhat higher activity. Since the exact structure of the anion involved with MAO/TBP activation is unclear, it is difficult to understand if and how the anion plays a direct role in the C2x–C2 isomerization process.

(48) (a) Beringhelli, T.; D'Alfonso, G.; Maggioni, D.; Mercandelli, P.; Sironi, A. *Chem. Eur. J.* **2005**, *11* (2), 650. (b) Beck, S.; Lieber, S.; Schaper, F.; Geyer, A.; Brintzinger, H.-H. *J. Am. Chem. Soc.* **2001**, *123* (7), 1483.

(49) Zucchini, U.; Albizzati, E.; Giannini, U. *J. Organomet. Chem.* **1971**, *26* (3), 357.

(50) (a) Ahlrichs, R.; Bär, M.; Baron, H.-P.; Bauernschmitt, R.; Böcker, S.; Ehrig, M.; Eichkorn, K.; Elliott, S.; Furche, F.; Haase, F.; Häser, M.; Hättig, C.; Horn, H.; Huber, C.; Huniar, U.; Kattannek, M.; Köhn, A.; Kölmel, C.; Kollwitz, M.; May, K.; Ochsenfeld, C.; Ohm, H.; Schäfer, A.; Schneider, U.; Treutler, O.; Tsereteli, K.; Unterreiner, B.; von Arnim, M.; Weigend, F.; Weis, P.; Weiss, H. *Turbomole Version 5*; Theoretical Chemistry Group, University of Karlsruhe, Karlsruhe, Germany, 2002. (b) Treutler, O.; Ahlrichs, R. *J. Chem. Phys.* **1995**, *102* (1), 346.

(51) (a) PQS, version 2.4; Parallel Quantum Solutions, Fayetteville, AK, 2001 (the Baker optimizer is available separately from PQS upon request). (b) Baker, J. *J. Comput. Chem.* **1986**, *7* (4), 385.

(52) Eichhorn, K.; Treutler, O.; Öhm, H.; Häser, M.; Ahlrichs, R. *Chem. Phys. Lett.* **1995**, *242* (6), 652.

(53) (a) Becke, A. D. *Phys. Rev. A* **1988**, *38* (6), 3098. (b) Perdew, J. P. *Phys. Rev. B* **1986**, *33* (12), 8822.

(54) Schäfer, A.; Horn, H.; Ahlrichs, R. *J. Chem. Phys.* **1992**, *97* (4), 2571.

(55) Andrae, D.; Häussermann, U.; Dolg, M.; Stoll, H.; Preuss, H. *Theor. Chim. Acta* **1990**, *77*, 123.

(56) Frequencies below a threshold of 11 cm⁻¹ were smoothly adjusted to a value remaining above 10 cm⁻¹ to avoid artificial “blow-up” of the entropic correction for very low frequencies, for which the harmonic oscillator model is no longer appropriate.

(57) Schäfer, A.; Klamt, A.; Sattel, D.; Lohrenz, J. C. W.; Eckert, F. *Phys. Chem. Chem. Phys.* **2000**, *2*, 2187.

(58) Shao, Y.; Molnar, L. F.; Jung, Y.; Kussmann, J.; Ochsenfeld, C.; Brown, S. T.; Gilbert, A. T. B.; Slipchenko, L. V.; Levchenko, S. V.; O'Neill, D. P.; DiStasio, R. A., Jr.; Lochan, R. C.; Wang, T.; Beran, G. J. O.; Besley, N. A.; Herbert, J. M.; Lin, C. Y.; Van Voorhis, T.; Chien, S. H.; Sodt, A.; Steele, R. P.; Rassolov, V. A.; Maslen, P. E.; Korambath, P. P.; Adamson, R. D.; Austin, B.; Baker, J.; Byrd, E. F. C.; Dachsel, H.; Doerksen, R. J.; Dreuw, A.; Dunietz, B. D.; Dutoi, A. D.; Furlani, T. R.; Gwaltney, S. R.; Heyden, A.; Hirata, S.; Hsu, C.-P.; Kedziora, G.; Khalliulin, R. Z.; Klunzinger, P.; Lee, A. M.; Lee, M. S.; Liang, W. Z.; Lotan, I.; Nair, N.; Peters, B.; Proynov, E. I.; Pieniazek, P. A.; Rhee, Y. M.; Ritchie, J.; Rosta, E.; Sherrill, C. D.; Simmonett, A. C.; Subotnik, J. E.; Woodcock, H. L., III; Zhang, W.; Bell, A. T.; Chakraborty, A. K.; Chipman, D. M.; Keil, F. J.; Warshel, A.; Hehre, W. J.; Schaefer, H. F.; Kong, J.; Krylov, A. I.; Gill, P. M. W.; Head-Gordon, M. *Phys. Chem. Chem. Phys.* **2006**, *8*, 3172.